Small-Angle Neutron Scattering Study of Polyethylene-*co*-Methacrylate Ionomer Aqueous Solutions

Gérard Gebel* and Benoit Loppinet

Département de Recherche Fondamentale sur la Matière Condensée, SI3M/Groupe Polymères Conducteurs Ioniques, CEA-Grenoble, 17, rue des Martyrs, 38054 Grenoble Cedex 9, France

Hisaaki Hara and Eisaku Hirasawa

Technical Center, Dupont Mitsui Polychemicals Co. Ltd., 6, Chigusa-Kaigan, Ichiara-shi, Chiba-ken 299-01, Japan

Received: November 27, 1996; In Final Form: March 4, 1997[⊗]

A small-angle neutron scattering (SANS) study of aqueous solutions of polyethylene-*co*-methacrylic acid partially neutralized ionomers is presented. A series of polymers presenting different degrees of polymerization, degrees of neutralization, counterions, and molecular weights are studied. The modeling of the dilute solution spectra combined with the analysis of the large-angle asymptotic behavior of the concentrated solutions spectra allowed us to conclude that these polymers form very large colloidal particles which are well described as either finite length cylinders or prolate ellipsoids. It is shown that the most important parameter defining the size of the particles is the ionic content. The radius varies from 55 to 135 Å and is proportional to the average distance between ionized carboxylated groups while the length of the particles increases dramatically for low ionic content. A transition from almost spherical particles to cylinders was evidenced. The effect of the concentration and of the molecular weight can be considered as negligible while the effect of the counterion is a modification of the eccentricity of the particles. The SANS spectra of concentrated solutions present a well-defined maximum. The position of the scattering maximum can be calculated using space-filling arguments, and the shape of the interference term is well reproduced by a Hayter and Penfold analysis.

Introduction

The structure of ionic polymer solutions in polar solvents depends on the ionic content along the polymer chain and on the ability of the solvent to dissolve the neutral polymer analogue. At one extreme hand the polyelectrolytes, which contain around one ionic group per monomer, are readily soluble. The solutions are characterized by more or less stretched polymer chains due to the electrostatic repulsions between ionic groups.[1] On the other hand, ionomers contain only few ionic groups along the polymer chain (<15 mol %) and were extensively studied as bulk materials or swollen ion-exchange membranes due to their industrial interest.[2,3] Most of the studies devoted to ionomer solutions have been performed in either polar or apolar solvents which are able to solubilize the neutral analogue polymer in order to elucidate the effect of the presence of few ionic groups along the polymer chain on the structure and properties of polymer solutions.[4−6] The results indicated a weakly charged polyelectrolyte behavior in polar solvents and the existence of polymer chain aggregation in apolar solvents due to the attraction of the non-ionized ion pairs.[7,8] Only few studies have been devoted to ionomer solutions in polar solvent which are poor solvent of the neutral polymer chain, mainly because of the difficulty to dissolve the polymer. The distance between ionic groups along the polymer chain combined with the nonsolubility of the hydrophobic polymer chain should induce a polymer chain aggregation in order to minimize the polymer−solvent interfacial energy. A colloidal structure was thus expected with particles composed of a polymer core and the ionic groups located at the polymer−solvent interface. The shape and the size of these "polymeric micelles" should be mainly related to the ionic content but also to the chemical structure and to the molecular weight of the ionomer. The discovery of a dissolution method for perfluorinated ionomers,[9] using mixtures of solvents and high temperatures, allowed the study of this new category of ionic polymer solutions. The existence of a colloidal structure due to the polymer chain aggregation was first evidenced by small-angle scattering studies.[10−12] The particles were shown to be rodlike with a radius around 20 Å and a length larger than 400 Å. The colloidal structure of aqueous perfluorinated ionomer solutions was confirmed by ESR and NMR measurement.[13,14] Another system belonging to this category of ionomer solutions (the poly(styrene−sodium 2-acrylamido-2-methylpropanesulfonate) solutions in *N*-methylformamide) appeared in the literature,[15] and an aggregation behavior was evidenced by light and X-ray scattering but the structure was analyzed in terms of the models developed for bulk ionomers.

The polyethylene-*co*-methacrylic acid partially neutralized ionomers (pEMAA) are together with the perfluorinated ionomers one of the most industrially used ionomers, the former as bulk materials for their interesting mechanical properties and the latter as ion-exchange membranes. Recently, DuPont-Mitsui Polychemicals Co. has developed a dissolution method for low molecular weight pEMAA ionomers in water.[16] A preliminary small-angle neutron-scattering (SANS) study has provided evidence for the colloidal nature of these solutions.[17] The aim of this work is to confirm the colloidal structure of these solutions, to determine the shape and the size of the particles and to study the effect of different parameters on the dimensions of the particles. For this purpose, solutions of polymers presenting different degrees of polymerization, degrees of neutralization, counterions, and molecular weights were studied in this work by SANS.

[⊗] Abstract published in *Advance ACS Abstracts,* April 15, 1997.

S1089-5647(96)03937-5 CCC: $14.00

TABLE 1: Characteristics of the pEMAA Ionomers[a]

samples	*E* (wt%)	MMA (wt %)	MFR (g/min)	cation	ionization (%)	v_0 (Å^3)	*N*
S1	85	15	60	Na	50	1960	72.8
S2	80	20	60	Na	50	1470	52.6
S3	80	20	300	Na	50	1470	52.6
S4	80	20	650	Na	50	1470	52.6
S5	80	20	60	K	50	1470	52.6
S6	80	20	300	K	50	1470	52.6
S7	80	20	650	K	50	1470	52.6
S8	85	15	60	Na	60	1634	60.7
S9	80	20	60	K	90	735	29.2

[a] *E* and MA correspond to the weight percent of monomers, MFR is the melt flow rate, v_0 is the average volume per ionized group, and *N* is the average number of CH_2 between two ionized groups.

Experimental Section

pEMAA ionomers are copolymers of ethylene and methacrylic acid:

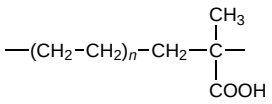

Aqueous solutions containing around 25 w/w% of polymer were provided by DuPont-Mitsui Polychemicals Co. (Japan). The solutions were obtained by dissolution in an autoclave in water under stirring (1200 rpm) at 130−150 °C for 30 min.[16] The neutralization, using the appropriate quantity of NaOH (or KOH), was performed either before (S8) or during the dissolution process (S1−S7, S9). The neutralization degrees presented are calculated values assuming complete reaction. Some characteristics of the polymers are given in Table 1 including the degree of polymerization, the degree of neutralization, the counterion, the average number of CH_2 between two ionized carboxylated groups (*N*), the average polymer volume associated with one ionized group (v_0), and the melt flow rate (MFR). The *N* and v_0 values were calculated assuming a statistical copolymerization and neutralization of the polymers. The MFR, measured on the non neutralized polymers by a melt indexer at 190 °C under a 2160 g load, is a good indication of the relative molecular weights; i.e., the higher is MFR value, the lower the molecular weight.

In this work, we have mainly focused our study on the structure of the S8 and S9 solutions. The main difference between the two polymers is the ionic content. The average number of CH_2 between two ionized carboxylic groups is statistically 60 and 29 for the S8 and S9 polymers, respectively. It follows that the S8 particles were expected to be roughly twice as large as those encountered in the S9 solutions. The effect of the other structural parameters were deduced studying the following series of ionomers:

(i) The S2, S3, and S4 polymers presenting increasing MFR values allowed us to study the effect of the molecular weight. The same analysis was performed with the series S5, S6, and S7.

(ii) The effect of the counterion was deduced comparing S2 to S5, S3 to S6, and S4 to S7.

(iii) The comparison between S1 and S8 ionomers gave information on the effect of the degree of neutralization.

Molecular weight distributions were measured for some base copolymers on the nonneutralized form using GPC. The average molecular weights are $M_n = 19\,200$ ($M_w = 94\,500$) for the S1 and S8 polymers and $M_n = 10\,100$ ($M_w = 37\,500$) for the S3 and S6 polymers. The large molecular weight polydispersity is due to the industrial origin of the base copolymers. The MFR values of the S8 and S9 polymers are identical, indicating that the molecular weights of the two polymers are very close. The density of the polymer in solution was assumed to be identical to the bulk density (0.96 g/cm^3) in accordance with measurements of the density performed on concentrated solutions in heavy water. The solutions were dialyzed in deuterated water in order to obtain a good contrast for SANS experiments. Concentrations were measured by evaporation and weighing after dialysis. Various concentrations were then prepared by volume dilution. Further check of dialyzed solutions by ^{1}H NMR using a Brucker AC200 indicated that the level of remaining protonated water was negligible for SANS experiments (<1%).

A dilution of the starting solution was observed during the dialysis process. This dilution is attributable to an effect of the osmotic pressure in the limit of the swelling of the dialysis bag and to the fact that the dialysis bags were not completely impermeable to the polymer particles. Such permeation was observed since pEMAA solutions present a milky appearance and the outer solutions slightly scatter light. After 3 days of dialysis, the outer solution contained less than 1% of starting quantity of the polymer. Two 5% S8 solutions were prepared by D_2O dilution of the dialyzed solution and of the starting H_2O solution. The SANS spectra obtained with these solutions were exactly superimposable over the entire angular once normalized by the contrast variation taking into account the presence of a H_2O volume fraction of 16.7% in the sample prepared by D_2O dilution of the starting H_2O solution. This result indicates that the dialyzed solution can be considered as identical with the original solution, namely, the particle size distribution is not significantly modified during the dialysis process at least as observed by SANS.

The SANS experiments were performed on the PAXE spectrometer at the Laboratoire Léon Brillouin (Orphée reactor, Saclay, France). The total angular range was accessed using several different configurations varying from $0.02 < q(\text{Å}^{-1}) < 0.4$ ($\lambda = 5$ Å, $D = 1.2$ m) to $0.005 < q(\text{Å}^{-1}) < 0.08$ ($\lambda = 12$ Å, $D = 5$ m) where λ is the wavelength, *D* is the sample-to-detector distance, *q* is the momentum transfer ($q = 4\pi \sin\theta/\lambda$) and 2θ is the total scattering angle. Experiments were carried out using quartz cells with a 1 mm path length. For concentrated solutions, a multiple scattering effect was evidenced, and the spectra were then recorded using thinner cells (0.1 mm). The usual corrections for background and incoherent scattering subtraction and transmission correction were applied. The absolute intensity calibration was performed by the determination of the incident flux during transmission measurements.[18]

Results and Discussion

The SANS spectra corresponding to S8 and S9 pEMAA concentrated solutions in D_2O obtained from dialysis ($\phi = 22\%$ and $\phi = 21\%$, respectively) over the entire angular range are presented on Figure 1. The main features of these spectra, clearly visible on Figure 1 are (i) the very large values of the scattered intensities, (ii) the existence of a well-defined maximum located at low *q* values, and (iii) a q^{-4} behavior of the scattered intensities at large *q* values. As a first approach, the position of the scattering maximum can be related to an average distance between scattering objects. The very large interparticle distance deduced from the low-*q* position of the scattering maximum when combined with a concentration larger than 20% has to be interpreted as originating from very large particles. The scattered intensities, expressed in cm^{-1}, are proportional to a contrast factor ($(\Delta\rho)^2 \approx 4 \times 10^{21}$ cm^{-4} depending on the polymer), to the polymer volume fraction and to the volume of

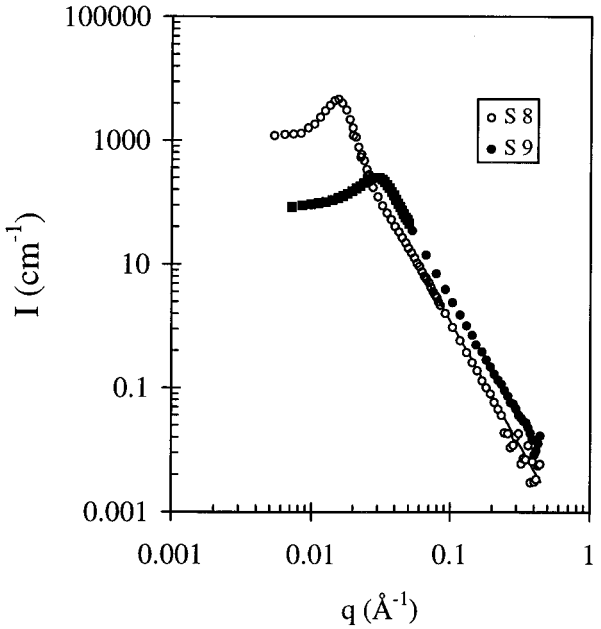

Figure 1. SANS spectra for the S8 (○) and S9 (●) concentrated solutions (respectively $\phi = 22\%$ and $\phi = 21\%$).

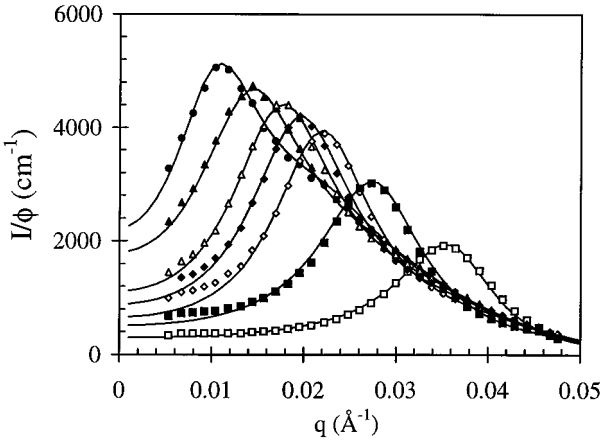

Figure 2. SANS spectra for S9 solutions $\phi = 20.4\%$ (□), 9.5% (■), 4.9% (◇), 3.4% (◆), 2.4% (Δ), 1.2% (▲) and 0.7% (●). The solid lines correspond to calculated curves using the Hayter and Penfold method.

the scattering particles. The very high level of scattered intensities can also be correlated to the existence of very large particles. The intensity scattered at large angles gives information on the surface of the scattering objects. A q^{-4} behavior indicates the existence of a sharp interface between the particle and the solvent.[19] These characteristics are typical of colloidal dense particles. They were observed whatever the concentration and the polymer. The differences between the scattered intensities and the peak positions observed for the S8 and S9 solutions for similar concentrations clearly indicate that the S8 particles are significantly larger than the S9 particles.

The position of the scattering maximum shifts toward smaller q values on decreasing the concentration as presented on Figure 2 for the S9 polymer solutions. The evolution of the Bragg distance deduced from the peak position, $d_{max} = 2\pi/q_{max}$, with the polymer volume fraction presents a linear trend on a double-logarithmic plot for both the S8 and the S9 solutions (Figure 3). The slope is identical for the two solutions and corresponds to a tridimensional dilution (d_{max} is proportional to $\phi^{-1/3}$). This indicates that none of the dimensions of the scattering particles is extremely large compared to the interparticle distance even in the most concentrated solutions. The same study performed

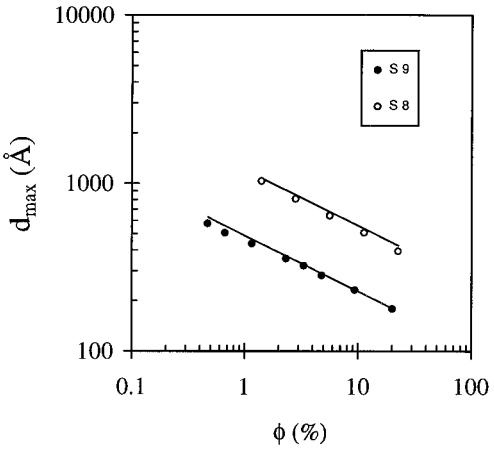

Figure 3. Dilution laws for the S8 (○) and S9 (●) polymers. The solid lines correspond to calculated curves using space filling arguments.

with perfluorinated ionomer solutions in various solvents leads to a bidimensional dilution (d_{max} is proportional to $\phi^{-1/2}$).[10,11] Therefore, in contradistinction to perfluorinated ionomers, the S8 and S9 pEMAA solutions do not contain very long cylindrical particles.

The scattering invariant for a two-phase system is defined as

$$INV = \int_0^\infty q^2 I(q)\, dq = (\Delta\rho)^2 \phi(1-\phi) 2\pi^2 \qquad (1)$$

where ϕ is the polymer volume fraction and $\Delta\rho$ the scattering length density contrast between the particle and the solvent. Neutron-scattering intensities were determined on an absolute scale which allows the comparison between the experimental value determined by the q integration of the scattering curve and the calculated value using the contrast determined from the chemical formula. The comparison between the two values leads to an excellent agreement; for example, $INV_{exp} = 1.35 \times 10^{22}$ cm^{-4} and $INV_{calc} = 1.43 \times 10^{22}$ cm^{-4} for the spectrum of the S8 solution presented on Figure 1. The same quality of agreement was obtained for all the polymers and all the concentrations. This result, combined with the q^{-4} behavior observed for all the spectra, is evidence that the solution is a true two-phase system and suggests that no solvent penetrates the particles as observed for the perfluorinated ionomers.[11]

This result was then confirmed by a polymer−solvent contrast variation experiment. Concentrated S8 solutions ($\phi = 10\%$) were prepared mixing H_2O and D_2O S8 solutions. The spectra appeared then to be proportional over the entire angular range whatever the D_2O/H_2O ratio. For colloidal systems, the scattered intensity can be considered as a combination of a term depending only on the shape of the particles, $F(q)$ is called the form factor, and of a term related to the spatial distribution of the scattering objects, $S(q)$ is called the interference term. The distribution of the particles is expected to be independent of the isotopic composition of the solvent. Therefore, any modification of the spectra depending on the D_2O/H_2O ratio has to be related to the apparent shape and dimension of the particles depending on the solvent scattering length density. The absence of modification of the scattering spectra depending on the D_2O content indicates that the particles present a constant scattering length from the center of the core to the surface. The intensity scaling factor with respect to the scattering curve obtained for the D_2O solution was determined for each D_2O/H_2O composition. The evolution of the square root of the scaling factor against the scattering length density of the D_2O/H_2O solvent mixture is linear as presented on Figure 4. The contrast match point, defined as the D_2O/H_2O composition

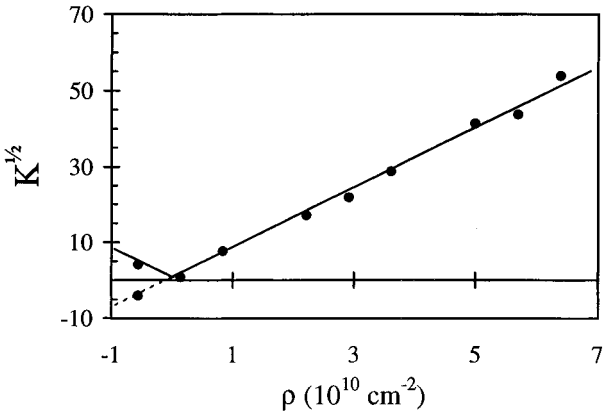

Figure 4. Evolution of the square root of the scaling factor vs the scattering length density of the D_2O/H_2O mixture.

where the scattering length densities of the particles and of the solvent are equal, was easily determined. The experimental scattering length density of the particles, $\rho_{exp} = 0.05 \times 10^{10}$ cm^{-2}, is in excellent agreement with the calculated value ($\rho_{calc} = -0.09 \times 10^{10}$ cm^2).

At low concentrations, the interparticle distance is large enough to avoid any contribution of the interference term in the explored q range ($S(q) \approx 1$). The observed scattered intensity can thus be considered as arising only from the form factor of isolated particles. For the S9 solution, the scattering maximum is visible on the spectra for a 0.7% solution. A dilution by a factor of 200 ($\phi = 0.09\%$) of the starting solution was necessary to eliminate the contribution of the scattering peak, and the same concentration was used for the S8 solution. In both cases, a spectrum for a lower concentration was recorded, and the spectra appeared exactly superimposable when normalized by the concentration, indicating that the effect of the interference term is negligible in the observed q range. Such study was possible only because the scattered intensity is very large due to the contrast factor and the size of the particles. The shape of the scattering curves cannot be reproduced using the theoretical form factor of monodisperse spherical particles. Both the absolute intensities and the shape of the curves can be fitted using the form factor of either finite length cylinders or prolate ellipsoids. The theoretical intensities for finite length cylinders, expressed in cm^{-1}, are calculated using the following relation:

$$\frac{I(q)}{\phi} = (\Delta\rho)^2 \cdot 4V \cdot \int_0^1 \left[\frac{\sin(qLu)}{qLu} \frac{J_1(qR\sqrt{(1-u^2)})}{qR\sqrt{(1-u^2)}}\right]^2 du \quad (2)$$

where J_1 is the first-order Bessel function, V, L and R are the volume, the semilength and the radius of the cylinders, respectively. For prolate ellipsoids, the following expression was used:

$$\frac{I(q)}{\phi} = (\Delta\rho)^2 \cdot V \cdot \int_0^1 \left[3\frac{\sin(qu) - qu\cos(qu)}{(qu)^3}\right]^2 dx \quad (3)$$

with

$$u = \sqrt{(ax)^2 + b^2(1-x^2)} \quad (4)$$

where a and b are respectively the semiminor and the semimajor axis.

The results obtained for the radius and the semilength of cylinders and for the semiminor and -major axes of prolate ellipsoids are given in Table 2. The best fit using the form factor of a prolate ellipsoid is presented for the S8 solution on Figure 5. The agreement over 6 orders of magnitude in intensity between the theoretical and the experimental scattering curves is excellent for both the absolute intensities and the shape of the scattering curve. The theoretical form factor presents numerous oscillations at large angles which are severely damped in the experimental curve due to size polydispersity. However, the first oscillation, whose position is strongly sensitive to the fit parameters, is clearly visible on the spectrum and is well reproduced by the theoretical form factor. It is worth noting that the only difference between form factors of prolate ellipsoids and finite length cylinders presenting the same volume and the same surface appears in the level of the minima observed at large angles. The absence of marked minima in the experimental spectra does not allow a choice between these two geometries. The low eccentricity of the particles combined with the absence of abrupt angles favors the ellipsoidal geometry. However, the smallest dimension of the particles should be determined by the energy minimization between the polymer/solvent interfacial energy and the elastic polymer chain energy which are stretched in order to locate the ionic groups in the polar medium. These energetic arguments should favor the cylindrical shape presenting a smaller minor dimension compared with ellipsoids. The actual geometry should be in between the ellipsoidal and the cylindrical geometries. The same arguments can be used to reject the distribution of spheres. A distribution of spherical particles reproducing the scattering curves can always be found but such distribution will necessarily include large particles which are not energetically favored.

The asymptotic behavior of the scattering curves scales as q^{-4} at large q values over at least one decade in q (Figure 1) which indicates that the particles present a sharp interface. Such q^{-4} behavior is observed for all the polymers and all the concentrations. The Porod representation ($q^4I(q)$ vs q plot)

TABLE 2: Results of the Best Fits for the Ellipsoidal and Cylindrical Geometries[a]

	S1	S2	S3	S4	S7	S8	S9
ellipsoid							
a (Å)		105	105	104	112	124	59
b (Å)		420	305	320	230	355	105
cylinder							
R (Å)	135	99	101	98	105	115	55
$2L$ (Å)		321	230	230	160	260	80
σ (Å^2)	26.1	34.3	33.9	36.4	37.19	35.5	35.9
D (Å)	92.8	67.0	67.0	67.0	67.0	77.4	37.4
$2R/D$	2.91	2.96	2.93	2.93	3.13	2.97	2.94

[a] a and b are the semiminor and -major axis, R and L are the radius and the semilength for cylinders, σ is the area per polar head, D is the calculated average distance between ionic groups.

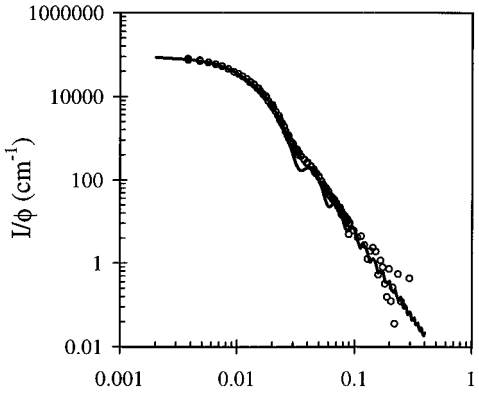

Figure 5. SANS spectrum of a dilute S8 solution ($\phi = 0.09\%$). The solid line corresponds to the best fit for an ellipsoidal shape ($a = 124$ Å, $b = 355$ Å).

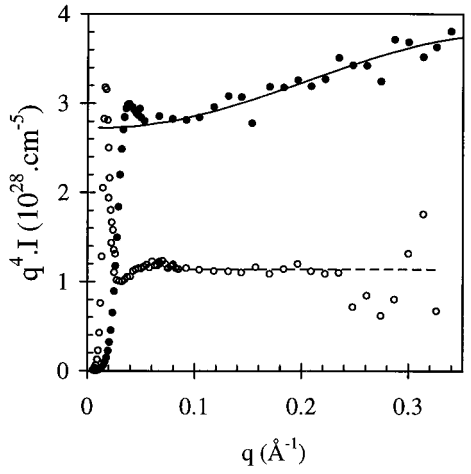

Figure 6. Porod plot for the spectra of Figure 1. The solid line corresponds to the best fit obtained using eq 7 ($d = 8$ Å, $\rho_{shell}/\rho_{core} = 1.08$).

allows extraction of the so-called Porod limit which relates the level of scattered intensity at large q values to the surface over volume ratio:

$$\lim_{q\to\infty} q^4 I(q) = 2\pi(\Delta\rho)^2\Sigma \qquad (5)$$

where Σ is the total surface over volume ratio. The Porod plots obtained for an S8 and an S9 solution are presented in Figure 6. A constant background due to the hydrogenated part of the polymer was subtracted according to a standard procedure.[20] The Porod limit was extracted without any difficulty for the S8 polymer. The scattering curves normalized by the polymer volume fraction present the same Porod limit at large q values whatever the concentration. Therefore, the surface over volume ratio per particle is constant strongly indicating that the shape and the dimensions of the scattering particles are not modified with dilution. The experimental value of the surface over volume ratio per scattering particle for the S8 solution ($\Sigma_{exp}/\phi = 1.92 \times 10^{-2}$ Å^{-1}) deduced from the Porod limit on figure 6 using $(\Delta\rho)^2 = 41.4 \times 10^{20}$ cm^{-2} and $\phi = 0.22$ can be compared to the one calculated for an ellipsoidal shape using the dimensions reported in Table 2 ($\Sigma_{calc}/\phi = 1.99 \times 10^{-2}$ Å^{-1}). The agreement is excellent between the determination using the Porod limit for a concentrated solution ($\phi = 22\%$) and the calculated value using the dimensions extracted from the fit of dilute solution spectra ($\phi < 0.1\%$) confirming that the particle dimensions are independent of the concentration.

The spectrum of the S9 solution exhibits a positive deviation from a constant value in a Porod representation (Figure 6). Positive deviations are usually attributed to a poorly subtracted background, but the observed deviation on Figure 6 extends over a too large q range to be corrected by a constant background subtraction. For colloidal particles, the commonly observed deviations from the Porod law are negative due to a diffuse interface.[21] A possible origin for the positive deviation can be the existence of a shell at the particles−solvent interface presenting a higher scattering length density, ρ_{shell}, compared to the particle core, ρ_{core}. In such a case, the Porod behavior can be described using[22]

$$q^4 I(q) = 2\pi\Sigma((\rho_{core} - \rho_{D_2O})^2 + (\rho_{shell} - \rho_{core})(\rho_{shell} - \rho_{D_2O})(1 - \cos(qd))) \qquad (6)$$

where ρ_{D_2O} is the scattering length density of the solvent and d is the thickness of the shell. The Porod behavior of the S9 solution can be reproduced with $\rho_{shell}/\rho_{core} = 1.08$ and $d = 8$ Å as presented on Figure 6. The experimental value of the surface over volume ratio, $\Sigma_{exp}/\phi = 4.83 \times 10^{-2}$ Å^{-1}, deduced from the fit of the curve at large q values using eq 6 compares well with the calculated value 4.89×10^{-2} Å^{-1}. This result is in agreement with the recent ESR study of the dynamics of the chain in the S9 particles using spin probes.[23] The authors deduced the existence of a 10 Å thick shell at the ionomer−solvent interface presenting a restricted mobility of the chains due to constraints arising from the presence of ionic groups in close proximity.

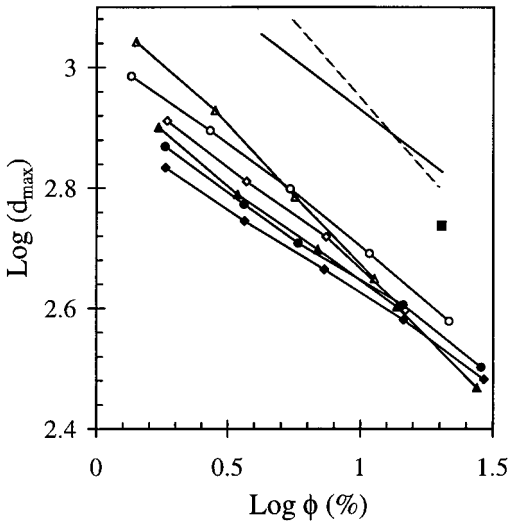

Figure 7. Dilution laws for the S1 (■), S2 (△), S3 (◇), S4 (○), S5 (full triangle), S6 (◆), and S7 (●) polymers. The two additional lines are a $\phi^{-1/3}$ (solid line) and a $\phi^{-1/2}$ (dashed line) dilution laws.

Dilution laws for the S2−S7 solutions are presented in Figure 7. Most of the peak positions scale as $\phi^{-1/3}$, except for the S2 solution which presents a bidimensional dilution law ($\phi^{-1/2}$). The existence of very long cylindrical particles in the S2 solution cannot thus be rejected. At large concentrations, a transition is also observed between a $\phi^{-1/3}$ and a $\phi^{-1/2}$ dilution law for the S5 solution. This similarity could be expected since the S2 and the S5 polymers were prepared from the same base copolymer. The spectrum obtained for the concentrated S1 solution presents a poorly defined scattering maximum located at too low q values to determine properly a dilution law. The molecular weight of the ionomer is probably not a relevant parameter defining the size of the particles since the dilution law observed for the S7 solution is located in between the S5 and S6 ones while the MFR value increases continuously from S5 to S7. For particles presenting the same aggregation number, space-filling arguments imply that the average distance between particles scales as the power one-third of their volume which must be proportional to the molecular weight. The peak positions obtained for the S5 and S6 polymers were thus expected to vary from 26% since their molecular weights differ roughly by a factor 2, but the experimental data vary less than 2% over the overall concentration range. It follows that the aggregation number cannot be constant and probably varies almost linearly with the molecular weight. The same conclusions were deduced comparing the S2, S3, and S4 solutions. The effect of the counterion is also rather small, but it appears that the peak positions for the S5, S6, and S7 solutions are systematically shifted to lower distance compared to the S2, S3, and S4 solutions. The S1 and S8 polymers were prepared from the same base polymer, and the only difference is the degree of neutralization. The scattering maximum is significantly shifted toward lower q values for the S1 concentrated

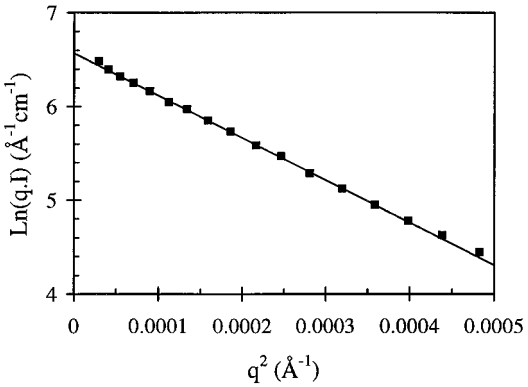

Figure 8. Guiner plot applied to cylindrical shape for the S1 solution ($\phi = 0.1\%$).

solution compared to the S8 solution indicating that larger particles are observed concomitant to an increase of the average distance between ionized carboxylated groups along the polymer chain.

The study of the dilute solutions was also performed for the S1, S2, S3, S4, and S7 polymers. The spectra obtained for S1 solutions does not present any deviation from the $1/q$ behavior at low q values indicating that no information can be obtained about the length of the particles from SANS experiments. The S1 dilute solution spectrum was then fitted using the Guinier approximation applied to homogeneous cylindrical particles:[19]

$$\frac{qI(q)}{\phi} = (\Delta\rho)^2\pi^2R^2\exp\left(-\frac{q^2R^2}{4}\right) \qquad (7)$$

The spectrum presented on a $\ln(qI)$ vs q^2 plot (Figure 8) is linear at low q values in the domain of validity of the eq 7 ($qR < 1.4$). Two values of the radius can be extracted from the slope and the extrapolation at zero q value. The two values (respectively $R = 133$ Å and $R = 136$ Å) are in good agreement and can be considered as an independent determination since the former is related to the shape of the scattering curve while the latter is related to its intensity. The large value of the radius explains that no information of the length can be obtained from the spectra since such information is be located at too low q values to be observable. The results obtained for the S2−S4 polymers solutions for both the cylindrical and the ellipsoidal geometries are presented in Table 2. The evolution of the dimensions confirms the statements deduced from the analysis of the dilution laws. The minor dimensions are found to be roughly constant for polymers presenting the same ionic content. This result confirms that the effect of the molecular weight is negligible. The radii of the particles increase when increasing the average distance between ionic groups. The S2 particles present a larger semi length compared to the S3 and S4 polymers explaining the existence of a transition of the dilution law from a $\phi^{-1/3}$ to a $\phi^{-1/2}$ behavior with increasing the concentration.

The spectra on a Porod plot present a well defined plateau and the oscillations of the theoretical form factor at large angles are severely damped indicating the existence of a large cross-sectional polydispersity. Such polydispersity is not surprising with materials which are far from being model compounds.

The dimension of the particles are very large compared to the maximum distance between ionized carboxylated groups which were calculated assuming a statistical distribution of the ionic groups along the polymer chain.[24] This distance, D, and the particle diameter over D ratio are given in Table 2. Despite the variation of the radius of the particles from 55 to 135 Å depending on the ionic content, the $2R/D$ ratio only varies from 2.9 to 3.1. This result indicates that the minor dimension increases linearly with the ionic content confirming that the distance between ionized groups is the relevant parameter in these systems. Two explanations can be proposed for the discrepancy between the diameter and the D value. Either the copolymerization and/or the neutralization are not statistical or two-thirds of the ionic groups are trapped inside the particles. Energetic arguments and the fact that the same $2R/D$ ratio is obtained for all the polymers does not favor the latter hypothesis.

Doubling the ionic content (S8 and S9 polymers) induces an increase by a factor 2 of the radius and by a factor larger than 3 of the length of the cylinders. This effect is partly attributable to the counterion effect as observed for the S4 and S7 polymers. The S4 and S7 polymers are similar except the counterion and the comparison between the dimensions of the particles indicates that the polymer particles on the K^+-neutralized form present a lower eccentricity and a slightly larger radius compared to the Na^+ form. The lower eccentricity of the particles is related to an increase of the area per polar head and explains that the transition from a $\phi^{-1/2}$ to a $\phi^{-1/3}$ dilution laws is shifted to larger concentrations for the S3 solution compared to the S2 solution.

While the radius increases almost linearly with the ionic content whatever the counterion and the molecular weight, the length of the particles increases much more dramatically. The effect is more pronounced comparing S1 and S8, a 10% increase of degree of neutralization induces a transition from a finite length cylinder to an apparently infinite one. A transition from an almost spherical particle (S9) to an infinite cylinder (S1) is observed when decreasing the ionic content.

The calculated volume of the S8 particles using the data of Table 2 is $V = 22.86\ 10^6$ Å^3. From the molecular weight by number $M_n = 19\ 200$, an average aggregation number can be calculated ($N_{agg} = 677$) assuming that the density corresponds to the bulk polymer. The calculated aggregation number for the S3 polymer is equal to 811 using $M_n = 10\ 100$ g/mol. These aggregation numbers are very large which explains that a modification of the molecular weight does not significantly modify the size of the particles as it appears in the values of Table 2 for the S2−S4 polymers. The influence of the molecular weight essentially affects the aggregation number. The molecular weight have not been yet determined for the other polymers, but an indication can be obtained comparing the MFR values. For example, the S8 and S9 polymers present the same MFR value, we can thus suppose that their molecular weights are similar. The volume of the S9 particles is 1.53×10^6 Å^3, which is 15 times lower than the one calculated for the S8 particles. Using 20 000 as molecular weight for the S9 polymer, a relatively low value of the aggregation number was obtained ($N_{agg} = 44$). The extrapolation of the evolution of the aggregation number depending on the ionic content suggests that, for an average number of CH_2 between two ionic groups around 10, the aggregation number will be close to 1 and the structure will be similar to that encountered in weakly charged polyelectrolyte solutions in a poor solvent.

The surface over volume ratio, Σ, is commonly used in the field of charged colloidal systems to determine the area per polar head, σ according to the relation

$$\sigma = \upsilon_0\left(\frac{2}{R} + \frac{1}{L}\right) = \upsilon_0\frac{\Sigma}{\phi} \qquad (8)$$

where υ_0 is the volume of the particle associated with one ionized carboxylate group. The areas per polar head are given in Table 2 and appear to be relatively constant indicating that the driving force defining the structure of the particles is the polymer−solvent interfacial energy as usually observed in

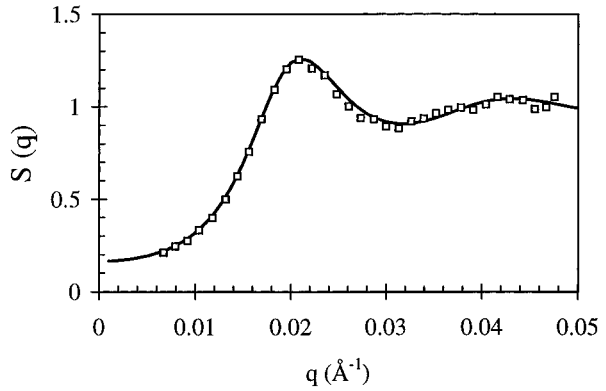

Figure 9. Interference term for a $\phi = 3.5\%$ S9 solution. The solid line was calculated according to the Hayter and Penfold method.

charged colloidal systems.[25] The only discrepancy is observed for the S1 solution due to the infinite length hypothesis ($1/L = 0$).

The origin of the maximum in the scattering curves of ionic polymer solutions has been subject of controversy. The two opposite models are based either on the existence of an ordering of the particles being limited to just a few neighbors or on the existence of a closest distance of approach between particles due to electrostatic repulsions (correlation hole model).[26,27] The easiest analysis is to consider that the scattering maximum originates from a local order between scattering particles and to use space-filling arguments. The maximum then corresponds to the first Bragg peak of the chosen array enlarged by the long-range disorder. The particles are highly repulsive and the array leading to the largest interparticular distance for a given density of scatterers is a compact array such as the face-centered cubic array. From the polymer volume fraction and the average volume determined from the dilute solutions analysis, a peak position can be calculated and compared to the experimental determination. The excellent agreement appears on Figure 3 despite the eccentricity of the particles.

Another analysis of the scattering maximum was developed for charged spherical particles by Hayter and Penfold.[28] They proposed a solution of the Orstein−Zernicke equation in the mean spherical approximation using a repulsive screened Coulomb potential in order to obtain an analytic form of the interference term. This model was developed for spherical particles, but such analysis could be successfully applied to ellipsoidal particles.[29] In this case, the interference term is calculated using the screened coulombic potential around the equivalent sphere. The Hayter and Penfold analysis was mainly developed for X-ray studies of micellar systems in which the contrast mainly arose from the hydrated ionic shell. In our neutron experiments, the contrast of the ionic shell is negligible compared to the contrast between the deuterated solvent and the polymer core as shown by the contrast variation experiment. The contrast factor was fixed as the value determined from the invariant analysis, $(\Delta\rho)^2 = 40.4 \times 10^{20}$ cm^{-2} for the S9 polymer. The equivalent radius was calculated from the volume of the particles and the theoretical form factor deduced from the fitting of the dilute solution spectra was used. The only parameter in the fitting procedure was thus the apparent ionic charge of the particle since the ionic shell was not considered. The result of the best fits are presented on Figure 2 for the S9 solutions and an example of the experimental interference term, obtained by division of the spectrum by the form factor, is compared to the interference term calculated by the Hayter and Penfold method on Figure 9. The agreement is excellent for a concentration range from 23% and 0.7% and the charge parameter was found to be roughly constant with values between 0.25 and 0.3 in this concentration range. This number can be due either to a counterion condensation or to the fact that part of the ionic groups are trapped inside the particles.

pEMAA ionomer solutions appear to behave similarly to PFSI solutions since colloidal solutions of elongated particles are observed. The dimensions of the pEMAA particles are independent of the concentration. Such behavior was already observed for perfluorinated ionomer solutions and was interpreted as a consequence of the dissolution at high temperature of these systems.[11] The energy necessary to form the particles from the bulk material is very large, and most of the parameters such as the concentration, the presence of added salt, the nature of the counterion and the solvent can produce only small modifications of the particle shape and size at room temperature. The analogy with PFSI solutions enables prediction of some behaviors for pEMAA ionomer solutions which will be verified in future experiments, namely, (i) the effect of the nature of the solvent will be very small acting through the interfacial energy and (ii) the effect of added salt will be only a decrease of the degree of ordering in the solution, no effects on the shape and the dimensions of the particles are expected.

PFSI materials are industrial materials and the effect of the distance between ionic groups could not been studied. Interest in the pEMAA ionomers arises from the possibility to monitor the ionic content acting on both the degree of copolymerization and the degree of neutralization. At low ionic content, the particles are cylindrical. Increasing the ionic content from 7.5 mol % (S1 polymer) to 18 mol % (S9 polymer) induces a transition from cylindrical to almost spherical particles. For ionic contents ranging from 20 to 40 mol %, the particles are expected to be spherical with a decreasing number of aggregation down to only one chain per particle. For ionic content larger than 50%, another transition is then expected from aggregated polymer chains in colloidal particles to isolated polymer chains for highly charged polymers.

Conclusions

The colloidal structure of the pEMAA solutions was evidenced by SANS. The particles were found to be very large and well described either by an ellipsoidal or a finite length cylindrical shape. The shape and dimension are shown to be independent of the concentration on a range from 25% to 0.1%. The dimensions of the particles were shown to be related to the ionic content along the polymer chain. The radius of the particle varies linearly with the average distance between ionic groups from 55 and 150 Å; however, the radius is 3 times larger than the average distance between ionic groups. The eccentricity of the particles increases dramatically when decreasing the ionic content and a transition from almost spherical particles to infinite cylinders is observed. Moreover the eccentricity was shown to be modified with the counterion. The effect of the molecular weight was shown to modify only the aggregation number which are found to be very large. The position of the scattering maximum was shown to be well reproduced by space filling arguments using a fcc array and the shape of the interference term can be reproduced by a Hayter and Penfold analysis.

Acknowledgment. We acknowledge the Laboratoire Léon Brillouin for neutron beam time and especially our local contact José Teixeira. We are also indebted to Thomas Zemb for the Hayter and Penfold analysis software and to T. Zemb, J. Lambard, and O. Spalla for fruitful discussions on the Porod behavior of the scattering curves.

References and Notes

(1) Oosawa, F. *Polyelectrolytes*; Marcel Dekker: New York, 1971.
(2) *Structure and properties of ionomers*; D. Reidel Publishing Co.: Dordrecht, Holland, 1987.
(3) *Ionomers : characterization, theory and applications*; CRC Press: Boca Raton, FL, 1996.
(4) Lundberg, R. D.; Phillips, R. R., *J. Polym. Sci.: Polym. Phys.* **1982,** *20*, 1143.
(5) Lantman, C. W.; MacKnight, W. J.; Higgins, J. S.; Peiffer, D. G.; Sinha, S. K.; Lundberg, R. D.; *Macromolecules* **1988**, *21*, 1339; *Macromolecules* **1988**, *21*, 1344.
(6) Hara, M.; Wu, J.; Lee, A. H. *Macromolecules* **1988**, *21*, 2214.
(7) Eisenberg, A.; Rinaudo, M. *Polym. Bull.* **1990**, *24*, 671.
(8) Gebel, G. *Macromolecular Complexes in Chemistry and Biology;* Dubin, P., Bock, J., Davies, R. M., Schulz, D. N., Thies, C., Eds.; Springer-Verlag, Heidelberg, 1994; p 329.
(9) Grot, W. G.; Chadds, C. European Patent 0 066 369, 1982.
(10) Aldebert, P.; Dreyfus, B.; Gebel, G.; Nakamura, N.; Pineri, M.; Volino, F. *J. Phys. (Paris)* **1988**, *49*, 2101.
(11) Loppinet, B.; Gebel, G.; Williams, C. E. *J. Phys. Chem.* **1997**, *101*, 1884.
(12) Gebel, G., Loppinet, B. *Ionomers: Characterization, theory and Applications*; Schlick, S., Ed.; CRC Press: Boca Raton, FL, 1996; Chapter 5, 83.
(13) Szajdzinska, E.; Schlick, S.; Plonka, A. *Langmuir*, **1994**, *10*, 1101; *Langmuir* **1994**, *10*, 2188.
(14) Schlick, S.; Gebel, G.; Pineri, M.; Volino, F. *Macromolecules* **1991**, *24*, 3517.
(15) Wang, J. W.; Wang, Z.; Peiffer, D. G.; Shuely, W. J.; Chu, B. *Macromolecules* **1991**, *24*, 790.
(16) Dupont Mitsui Polychemicals, Japanese patent, Tokkaihei 5-149908; Tokkaihei 5-286072.
(17) Gebel,G.; Loppinet, B. *J. Mol. Struct.* **1996**, *383*, 43.
(18) Cotton, J. P. *Neutron, X-rays and light scattering: Introduction to an investigate tool for colloidal and polymeric systems*; Lindner, P., Zemb, Th., Eds.; North Holland-Elsevier: Amsterdam, 1991; p 3.
(19) *Small-Angle X-ray scattering*; Glatter, O., Kratky, O., Eds.; Academic Press: London, 1982.
(20) Cabane, B.; Duplessix, R.; Zemb, T. *J. Phys. (France)* **1985**, *46*, 2161.
(21) Koberstein, J. T.; Stein, R. S. *J. Polym. Sci.: Polym. Phys.* **1983**, *21*, 2181.
(22) Auvray, L.; *C. R. Acad. Sci. Paris* **1986**, *302*, 861.
(23) Kutsumizu, S.; Schlick, S. *Macromolecules*, in press.
(24) Tanford, C. *J. Phys. Chem.* **1972**, *76*, 3020.
(25) Israelachvili, J. N.; Mitchell, D. J.; Ninham, B. W. *J. Chem. Soc., Faraday Trans. 2*, **1976**, *72*, 1525.
(26) de Gennes, P. G. *Ions in Macromolecular and Biological Systems*; Gregory, R. L., Ed.; Colston Papers, Vol. 29; J. Wright: Dorchester, 1978; p 69.
(27) Matsuoka, H.; Ise, N. *Adv. Polym. Sci*. **1994**, *114*, 187.
(28) Hayter, J. B.; Penfold, *Mol. Phys.* **1981**, *42*, 109.
(29) Hirata, H.; Hattori, N.; Ishida, M.; Okabayashi, H.; Frusaka, M.; Zana, R. *J. Chem. Phys.* **1995**, *99*, 17778.